Available online at www.sciencedirect.com
ScienceDirect
Proceedings of the Combustion Institute 33 (2011) 467–475
Proceedings of the Combustion Institute
www.elsevier.com/locate/proci

Experimental and computational study of oxidation of diethyl sulfide in a flow reactor

Xin Zheng [a], J.W. Bozzelli [b], E.M. Fisher [a,*], F.C. Gouldin [a], Li Zhu [b]

[a] Sibley School of Mechanical and Aerospace Engineering, Cornell University, Ithaca, NY 14853, USA
[b] Department of Chemistry and Environmental Science, New Jersey Institute of Technology, Newark, NJ 07101, USA

Abstract

The destruction of diethyl sulfide was studied experimentally and computationally at high temperatures under diluted oxidation conditions. The experiments were conducted in an atmospheric, turbulent flow reactor with a Reynolds number of around 5000, at four different operating temperatures between 630 and 740 °C. These oxidation experiments, with diethyl sulfide initially at approximately 100 ppm in the reactor, included near-stoichiometric conditions ($\Phi \sim 1$) and fuel-lean conditions with the equivalence ratio ($\Phi \sim 0.1$). On-line, radially extractive sampling in conjunction with fourier transform infrared spectroscopy and gas chromatography/mass spectrometry analysis was performed to quantify species at four locations along the centerline of the flow reactor. Species concentrations were presented as functions of residence time in the reactor and were compared to mechanism predictions. A previously published pyrolysis mechanism has been updated and extended to include kinetics of the partially oxidized intermediates. The new mechanism still reproduces the previously reported experimental pyrolysis results satisfactorily and provides reasonable agreement with experimental measurements for the present oxidation conditions. Important reactions were identified by sensitivity analysis and rate of production analysis by using the mechanism.

Keywords: Flow reactor; Oxidation; Probe sampling; Sulur-oxy-hydrocarbons; Thermochemistry

1. Introduction

Sulfur mustard (bis(2-chloroethyl) sulfide), also known as H/HD (military designation), is a primary component of the U.S. chemical warfare stockpiles [1]. As a lethal vesicant chemical, sulfur mustard is required to be destroyed under the Chemical Weapon Conventions [2]. In the U.S., incineration is employed as the baseline disposal technology due to its high destruction efficiencies, applicability to a wide range of chemicals, and good cost effectiveness. However, there has been strong public opposition to chemical weapons incineration because of concerns over trace level emissions from proper operation conditions as well as high level chemical release from off-design incineration modes [3]. In responding to the public concerns, great efforts have been put to investigate the destruction of chemical warfare agents under incineration-relevant conditions [4–6].

Experiments with actual sulfur mustard would provide the most direct insight into the thermochemical destruction of sulfur mustard. Because of the high toxicity of sulfur mustard, a simulant compound with related chemical structure is used

* Corresponding author. Address: Sibley School of Mechanical and Aerospace Engineering, 289 Grumman Hall, Cornell University, Ithaca, NY 14853, USA. Fax: +1 607 255 1222.
E-mail address: emf4@cornell.edu (E.M. Fisher).

1540-7489/$ - see front matter © 2010 The Combustion Institute. Published by Elsevier Inc. All rights reserved.
doi:10.1016/j.proci.2010.05.064

in the current study. The molecular structure of diethyl sulfide ($CH_3CH_2SCH_2CH_3$, abbreviation CCSCC) is similar to that of sulfur mustard but with ethyl rather than chloroethyl bonded to the sulfur atom. Diethyl sulfide has been investigated in several photolysis experiments [7,8], which show that the substitution of ethyl for chloroethyl does not change major reaction pathways under the conditions studied.

The present work continues the previous study on the pyrolysis of diethyl sulfide [9] by exploring the oxidation of diethyl sulfide. The experimental conditions were chosen to investigate the destruction of diethyl sulfide under incineration-relevant conditions and to understand the product formations under off-design modes. The experiments were complemented with mechanism development. The experimental data were used to validate and refine the mechanism. The goal of the present research has been to produce a kinetic mechanism of diethyl sulfide, which could be extended in the future to predict the behavior of sulfur mustard in incinerators.

2. Experimental apparatus and methodology

The details of the oxidation experiments are documented in [10] and briefly reviewed here. The experiments were conducted in an atmospheric turbulent reactor, consisting of a 4.5 cm ID × 100 cm long quartz liner inside a stainless steel pipe. The main carrier flow was preheated nitrogen. The secondary flow, diethyl sulfide and oxygen diluted in nitrogen, was injected into the main flow through four open-ended quartz tubes and resulted in a chemical loading 100 ± 4 ppm in the reactor. For experiments with approximately stoichiometric conditions ($\Phi \sim 1$), oxygen was provided from a pressurized cylinder ($21 \pm 0.2\%$ O_2 in N_2), while for the fuel-lean conditions ($\Phi \sim 0.1$), the oxygen was supplied in the form of on-site compressed air, purified by fourier transform infrared spectroscopy (FT-IR) purge gas generator (Whatman 75–51) to remove CO_2 and H_2O. Gas chromatography/mass spectrometry (GC/MS) analyses of samples taken just upstream of the injectors showed no evidence of reaction between diethyl sulfide and oxygen. Operating parameters are listed in Table 1.

Gas samples were extracted through radial sampling probes at four axial positions on the centerline of the reactor. The quartz sampling probes [10] make use of nitrogen dilution to quench reactions. Quenched gas samples were directed to FT-IR or GC/MS for analysis. Instrumental methods as well as species identification and quantification for each technique are the same as those of the pyrolysis study [9]. The uncertainties of species concentration are as follows: CCSCC (12%), ethylene C_2H_4 (5%), sulfur dioxide SO_2 (5%), carbon monoxide CO (5%), carbon dioxide CO_2 (5%), methane CH_4 (12%), ethane C_2H_6 (12%) and formaldehyde $CH_2{*}O$ (where $*$ represents a double bond) (15%).

Flow and temperature conditions are essential for interpreting experimental kinetic information. As shown in Table 1, the reactor flow was turbulent with a Reynolds number of approximately 5000 in all the operating conditions. Fig. S1, where S represent a Supplementary data, shows gas temperature profiles, consisting of an approximately isothermal region, the mean value of which is used to identify each operating condition, and a mixing region. Mixing conditions were determined in the pyrolysis experiment [9]. The mixing conditions for the current experiments are assumed the same as those of the pyrolysis experiments with the same flow rates and heater settings. The measured CO concentrations were used to correct species concentrations: the measured mole fraction of each species was multiplied by the ratio of the well-mixed CO concentrations to measured CO concentrations [9], to account for the effect of incomplete mixing.

3. Mechanism construction and computational method

The objective of the present work has been to develop thermochemistry of oxygenated sulfur-hydrocarbons and a kinetic mechanism that describes the destruction of diethyl sulfide under incineration-relevant conditions. The present chemical mechanism is constructed from the previous diethyl sulfide pyrolysis mechanism [9]; it includes updated thermochemistry and kinetics for a number of the pyrolysis reactions and the

Table 1
Experimental flow parameters and chemical loadings.

Nominal T (°C)	Main flow (slpm)	Secondary flow (slpm)	Velocity (m/s)	Re_D	O_2 loading (ppm)	CCSCC loading (ppm)
630	330	14.1	11.12	5020	730*/9321	100
670	341	15.3	12.02	5060	704*/9270	100
700	347	16.0	12.64	5060	720*/9366	100
740	350	16.8	13.30	4990	710*/9472	100

O_2 loadings with superscript '*' correspond to the conditions with approximately stoichiometric composition.

addition of new oxidation reactions and thermochemistry for oxygenated sulfur-hydrocarbons and sulfur oxides. The C–H–S–O mechanism used here consists of the following kinetic subsets: (1) reactions of diethyl sulfide and resulting sulfur intermediates, (2) reactions of small sulfur compounds, (3) hydrocarbon reactions, and (4) interactions between the first three subsets.

Kinetics of diethyl sulfide oxidation is a substantial component in the present work. The destruction of diethyl sulfide, through C–S bond cleavage and hydrogen abstraction by CH_3 and H, along with subsequent β-scission or isomerization of the resulting ethylthio (CCS$^{\bullet}$, where $^{\bullet}$ represents a radical site) and ethylthioethyl radicals (C$^{\bullet}$CSCC/CC$^{\bullet}$SCC) were published in the pyrolysis study [9]. Mechanism predictions were found to be highly sensitive to the kinetics of these reactions and thus a significant fraction of the kinetics and thermochemical properties have been refined using high accuracy ab initio and Density Functional Theory (DFT) calculations as described in a general review [11] and in [12–15] for similar sulfur containing species. Table S1 lists the previous kinetic parameters of these reactions as well as the current rates. In addition to the modifications, two new pyrolysis destruction routes for diethyl sulfide were added with the kinetics evaluated by the methods in [9]. These additional routes are: (1) unimolecular dissociation $CCSCC \leftrightarrow C_2H_6 + CH_3CH{*}S$ and (2) H addition to sulfur coupled with ethyl elimination $H + CCSCC \leftrightarrow CCSH + C_2H_5$. The updated mechanism reproduces the experimental pyrolysis results as satisfactorily as the previous mechanism [9] does, shown in Supplementary Fig. S2.

In this work, reactions of the diethyl sulfide and intermediates with O_2, OH, HO_2 and O were incorporated in the mechanism. These reactions are listed in order of occurrence during the destruction process as follows:

(1) H abstraction from CCSCC by O_2 as one of the initiation reactions.
(2) Destruction routes of CCSCC through (a) H abstraction by OH/HO_2/O, and (b) addition–elimination reactions via OH/O addition to the sulfur moiety and subsequent elimination of the ethyl group initially bonded to the sulfur. These addition/association reactions were in general exothermic or thermal neutral, as sulfur–oxygen bonds tend to be stronger than sulfur–carbon bonds.
(3) O_2 addition to ethylthio CCS$^{\bullet}$ and ethylthioethyl (C$^{\bullet}$CSCC/CC$^{\bullet}$SCC) radicals to form an adduct complex (peroxyl radicals), and subsequent reactions of the peroxyl radicals.
(4) Reactions of thioformaldehyde ($CH_2{*}S$) and thioacetaldehyde ($CH_3CH{*}S$). Three pathways are added for $CH_2{*}S$, one is H abstraction by OH, O or O_2, forming thioformyl (HCS) radical. Again OH/O/O_2 can associate at the radical site and undergo secondary isomerization or elimination resulting in $CH_2{*}O$ along with SH, S and SO, respectively, and the third is association reactions between thioaldehydes and their radicals to form sulfur dimer (S_2) and disulfides. Similar reactions are also included for thioacetaldehyde. As a more complex molecule, thioacetaldehyde can participate in multiple abstraction and β-scission steps as follows: (1) $CH_3CH{*}S + R \leftrightarrow C^{\bullet}H_2CH{*}S/CH_3C^{\bullet}{*}S + RH$, (2) $C^{\bullet}H_2CH{*}S/CH_3C^{\bullet}{*}S \leftrightarrow CH_2{*}C{*}S + H$, (3) $CH_2{*}C{*}S + R \leftrightarrow C^{\bullet}H{*}C{*}S + RH$, R=O/OH/H. Subsequent reactions with OH/O/HO_2 form HCO, HCS, CS and OCS. H atom can undergo addition to thioacetaldehyde and subsequent isomerization (intramolecular H transfer) to the carbon bonded to the sulfur forming the CCS$^{\bullet}$ radical. Similar addition routes are ignored for thioformaldehyde in the present mechanism, as the resulting methylthio ($CH_3S^{\bullet}$) is unstable and quickly returns to the reactants $H + CH_2{*}S$.

The kinetics of the small sulfur containing species derived from the reactions above, include HCS, CS, OCS, SH and S, are described in the small sulfur species subset of the mechanism. The kinetic and thermochemical basis for this subset is primarily the Leeds sulfur mechanism [16]. The reported work here extends it by (1) updating the kinetic parameters of H abstraction on HOSHO, as shown in Table S2, (2) extending reaction routes for species SOH/S/S_2/SO/SO_3/$HOSO_2$, (3) adding new species HSO_2, SOOH, CS, HCS, and COS and associated reactions. The subset consists of 21 species and more than 130 elementary reactions.

The kinetics for H abstraction from parent and intermediates by the radial pool in the two submechanisms above were from the formalism described in [17]. Association was treated as a chemical activation reaction with the kinetics evaluated by the methods in [11,18].

The hydrocarbon reaction subset in the present mechanism is a detailed mechanism for C_1, C_2 and C_3 hydrocarbons and oxygenated hydrocarbon species. The mechanism subset is constructed from hydrogen–oxygen–carbon monoxide chemistry at the base, with the reactions of larger species including CH_4, acetylene (C_2H_2), C_2H_4, C_2H_6, propyne (C_3H_4), propene (C_3H_6), propane (C_3H_8), and corresponding C_1, C_2 and C_3 aldehydes, alcohols and their reaction intermediates. The subset has been published in several parts in [18–28], and provided a basis for mechanism construction of JP-8 surrogate blends [29]. Validations against experimental data have been reported for opposed flow extinc-

tion experiments on ignition delay and flame speed measurements for several gaseous and liquid fuels [29] and for pyrolysis and oxidation of methanol and methanol/methane mixtures at temperatures 873–1073 K over a pressure range of 1–10 atm [30]. The present subset was adopted from [29]. For simplicity, reactions of nitrogen containing species, which are not likely to be significant under the present conditions, and reactions of C_4 and larger hydrocarbons which are formed in very minor quantities, are not included. The remaining hydrocarbon subset consists of approximately 450 elementary reactions among 150 species. The pyrolysis mechanism [9] included the hydrocarbon reactions that involved no oxygenated compounds. Three reactions in the hydrocarbon reaction subset, shown in Table S3, were updated with recent literature data [17,31,32].

Interactions between the subsets appear in two ways. One way is the coupling effect of major radicals such as H, O and OH between the reactions of the different subsets. For example, small sulfur chemistry may catalyze radical recombination [33] and thus affect the rates of radical attack on diethyl sulfide and other species. This cross-coupling mechanism is indirect, and does not require the addition of further reactions. The second way is through reactions between species in different subsets. The mechanism includes cross reactions between the diethyl sulfide submechanism and the hydrocarbon mechanism, specifically reactions of diethyl sulfide and its derivatives with CH_3 and C_2H_5. Kinetic parameters for those reactions were calculated by the same methods as described for the other subsets.

The thermochemical properties come from various sources. For most of the species included here, ab initio estimations at the CBS-QB3 level and DFT calculations [34] were carried out for products and adducts, and group additivity and hydrogen increment methods [35] were employed for radicals, when literature data are not available. Supplementary data 2 provides a table of enthalpies of formation, Entropy at 298 K and $C_p(T)$ from 300 to 1500 K. And Supplementary data 3 is a data table for coupling the species with Chemkin codes.

Chemical kinetic modeling was performed with the Chemkin 4 package [36]. The flow reactor was modeled as plug flow with smoothed gas temperature profiles (Supplementary Fig. S1) through curvefits to measured temperatures. Surface reactions were not included in the calculation.

4. Results and discussion

Mechanism predictions and experimental measurements of species profiles are shown in Figs. 1 and 2. The reported species, including CCSCC, C_2H_4, C_2H_6, CH_4, CO, CO_2, SO_2 and $CH_2{*}O$, were detected at levels of 1 ppm or higher in the experiments. Carbon disulfide (CS_2), ethyl methyl disulfide ($CH_3SSCH_2CH_3$), and diethyl disulfide ($CH_3CH_2SSCH_2CH_3$) were also detected and estimated to be below 1 ppm. In Figs. 1 and 2, experimental data are represented by symbols, while predictions by lines. As mentioned in Section 2, two analytical techniques were employed in the experiments. For species detected by both techniques, hollow symbols are for FT-IR measurements and solid symbols are for GC/MS measurements.

Figure 1 shows results with approximately stoichiometric composition at four temperatures, 630, 670, 700 and 740 °C. Repeatability is observed to be under the measurement uncertainties for duplicated measurements, and the results of the two different analytical techniques are in good agreement. Destruction efficiency of diethyl sulfide was experimentally determined to be 29% at 630 °C, 40% at 670 °C, 70% at 700 °C and 92% at 740 °C (the last sampling port), corresponding to residence times between 0.06 and 0.072 s. The mechanism prediction shows good agreement with the experiment for diethyl sulfide and C_2H_4 and CO under all these conditions. SO_2, $CH_2{*}O$, C_2H_6 and CH_4 are also quantified species, and their maximum concentrations are below 10 ppm. The mechanism overpredicts SO_2 at the 740 °C but underpredicts it at lower temperatures. $CH_2{*}O$ is underpredicted at all four operating temperatures. CH_4 and C_2H_6 are only quantified at the 700 and 740 °C, and are overpredicted in both temperatures.

Figure 2 presents results of the initial chemical composition with an equivalence ratio of about 0.1 at the 630, 670, 700 and 740 °C temperatures. As shown in Fig. 2, the destruction efficiency increases with temperature from approximately 34% at the 630 °C, to 60% at the 670 °C, 92% at the 700 °C, and 100% at the 740 °C (the last sampling port). In particular, at the 740 °C, complete destruction of diethyl sulfide is achieved by the second sampling port, corresponding to a residence time of 0.028 s. The destruction of diethyl sulfide is significantly enhanced with excess oxygen compared to the results in Fig. 1. The experimental profiles of CCSCC are in very good agreement with those of the mechanism prediction. For major species other than $CH_2{*}O$, the mechanism prediction agrees reasonably well with the measurement. Agreement is good for C_2H_4 and is fairly good for CO and SO_2 with small overpredictions at high residence times. $CH_2{*}O$ is underpredicted by factors up to 4. However, the use of a formaldehyde solution to calibrate the FT-IR for $CH_2{*}O$ introduces uncertainty regarding quantification of $CH_2{*}O$. Our measurements of $CH_2{*}O$ are considered upper bounds on mole fractions of the species, as $CH_2{*}O$ may polymerize in calibration gas transfer lines when it leaves the stabilized environment of the methanol

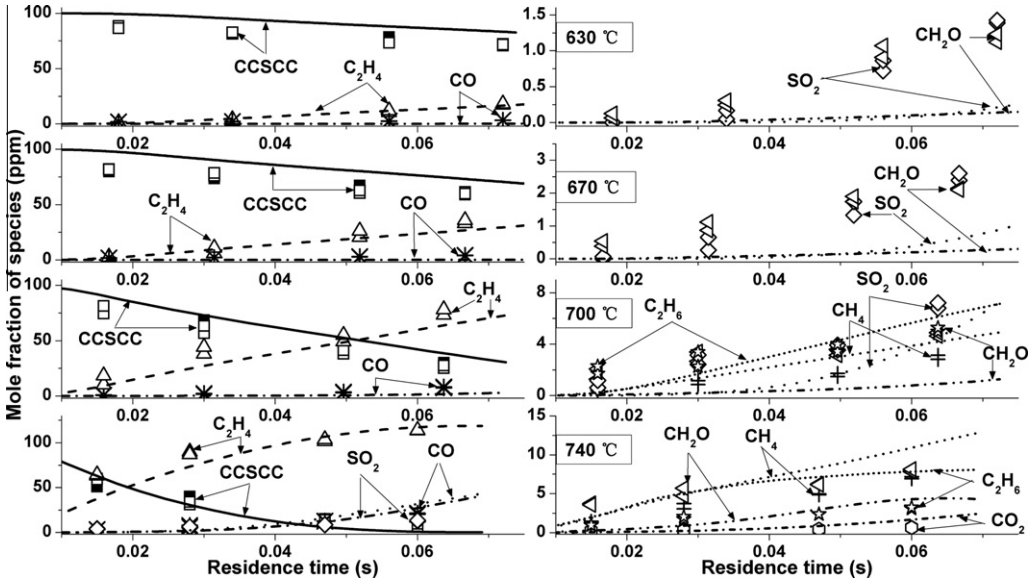

Fig. 1. Oxidation of diethyl sulfide with approximately 700 ppm O_2 loading.

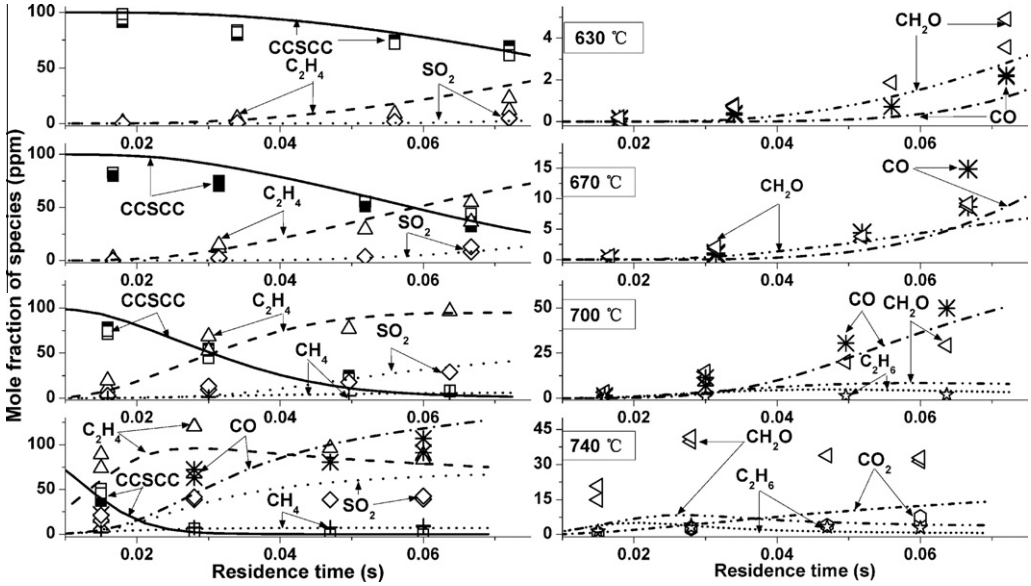

Fig. 2. Oxidation of diethyl sulfide with approximately 9000 ppm O_2 loading.

solution, producing overestimated concentrations in the calibration curve. Further investigations on $CH_2{*}O$ calibration would be valuable to improve the measurement accuracy on the species. C_2H_6 is only quantified at the 700 and 740 °C, and the predictions agree well with the experimental data. Oxidation of CO is not observed to be efficient under the conditions studied as CO_2 is quantified at the 740 °C, and is overpredicted with a maximum discrepancy of 30%.

In general, Figs. 1 and 2 show that the largest absolute disagreements between the measurements and calculations are in the single digit ppm range for CH_4, CO_2 and C_2H_6, and in the double digit ppm range for SO_2, $CH_2{*}O$, CCSCC, C_2H_4 and CO. These maximum discrepancies correspond to factors of ~2 for SO_2, CO_2 and $CH_2{*}O$, 60% for CH_4, and <40% for all other species. Possible explanations of the discrepancies observed in our study include: kinetic mechanism

error, reactions in sampling lines (either heterogeneous or due to non-instantaneous cooling) and deviation of the experiment from the modeled conditions (plug flow, uniform temperature, no wall reactions). This level of disagreement is very reasonable, given the state of the art of modeling the kinetics of simple systems containing sulfur, see for example [33].

In addition to the species reported above, light yellow condensates were observed on the internal surfaces of the sampling probes. The condensates were dissolved in methylene chloride, and the solution was analyzed by using GC/MS. Cyclooctasulfur (S_8) was identified as the major component, and a small unidentified peak was also present in the chromatogram.

As in our previous work [9], element balances show substantial gaps [10] due to the condensates above and to non-detectable species mentioned in the next section. Element balances range approximately from 65% to 90% for C, from 40% to 90% for H, and from 25% to 90% for S [10].

Rate of production analysis was conducted under several conditions to determine the reactions contributing significantly to the evolution of the parent compound and major species. The results for different temperatures and residence times are similar, and a representative case is shown in Fig. 3. Initiation of the destruction of diethyl sulfide in the present oxidation conditions is the same as that of pyrolysis study in [9], occurring through unimolecular dissociation. Reactions of H abstraction on diethyl sulfide by O_2 are included, but are not found to be a significant initiation source. Once the radical pool is established, abstraction reactions become important as chain propagation steps. The primary difference between oxidation and pyrolysis is the additional contribution of H abstraction by oxygenated reactants OH/O/HO_2/O_2. These reactions are more important under fuel-lean conditions with excess oxygen as they are more abundant. And among these reactions, abstraction by OH is the more important one as shown in Fig. 3. Water from the abstraction by OH is predicted to be an important species, but only very small amount was experimentally detected. Attempts to calibrate water have not been

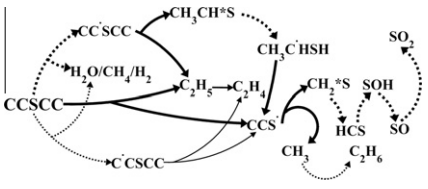

Fig. 3. Oxidation pathways of 100 ppm diethyl sulfide at the 740 °C with approximately 9000 ppm O_2 loading. Solid lines represent unimolecular dissociation, while dashed lines represent reactions involving other reactants. Line thickness indicates relative reaction rates.

successful to date. However, kinetic modeling showed that the predictions were not sensitive to the presence of H_2O, even at levels well above those believed present. H_2 is an important product from H abstraction but was not detectable by the instrumental methods used here. CH_4 is a minor detected species mainly formed through abstraction by CH_3.

The radicals derived from CCSCC are ethyl C_2H_5, ethylthio CCS· and primary and secondary ethylthioethyl C·CSCC/CC·SCC. These radicals undergo β-scission to produce C_2H_4, CH_2*S and CH_3CH*S, respectively. C_2H_4 is the primary hydrocarbon product, as shown in Figs. 1 and 2, detected under all the studied conditions. The CH_2*S and CH_3CH*S were not experimentally observed, probably because they are too unstable to survive the sampling lines [37]; however, anticipated polymerization products of these compounds were not detected in sampling line and probe rinsate. The primary pathway for thioformaldehyde is hydrogen abstraction to form HCS. In contrast, for thioacetaldehyde, H addition instead of H abstraction and subsequent isomerization to ethylthio CCS· is the most important route under all the conditions, while H abstraction and subsequent β-scission to thioketene CH_2*C*S become important at high temperatures under fuel-lean conditions. These gas phase reactions involving thioaldehydes, having been discussed so far, are however relatively slow at low temperatures. Thus high levels of thioaldehydes are predicted to persist to the exit of the reactor in the low temperature conditions studied here. The product, HCS radical undergoes the reaction with O_2 to form SOH, subsequent reactions with O and OH to sulfur monoxide (SO) and further oxidation results in SO_2. The other two detected species, C_2H_6 and CH_2*O, are mainly produced through the recombination of CH_3 and the reaction of CH_3 and O_2, respectively. In Fig. 3, oxidation of these hydrocarbons, which follows well known steps, is omitted.

Reactions of high importance in determining the mechanism prediction were determined through sensitivity analysis. Table 2 lists the top 10 reactions to which the concentrations of the major species, CCSCC, C_2H_4, CO, SO_2 and CH_2*O, are most sensitive for the condition of 740 °C with approximately 9000 ppm O_2 loading.

As seen in Table 2, the initiation reaction (simple C–S bond cleavage) has the highest sensitivity for all the listed species as it is the source of H which in turn affects concentrations of other important radicals, like OH and O, through fast chain propagation reactions. The rate constant for this reaction is obtained from the thermochemistry of the reaction system determined in this study, in combination with the QRRK [11]/master equation analysis [38] for pressure dependence (fall-off). The activation energy was calculated from the dissociation energy of the reaction using enthalpies of reactants and products calculated in this work. The

Table 2
Reactions with the highest sensitivity coefficient affecting the concentrations of major species at the 740 °C with approximately 9000 O_2 loading.

Reactions	Kinetic parameters			Sensitivity coefficient				
	A	N	E_a	CCSCC	C_2H_4	CO	SO_2	CH_2O
$CCSCC \leftrightarrow CCS^{\bullet} + C_2H_5$	1.06E + 89	−21.7	105718.0	−9.6	0.95	2.0	1.6	1.7
$CCSCC + H \leftrightarrow CC^{\bullet}SCC + H_2$	5.99E + 08	1.9	5141.0	−2.3	0.26	−0.42		−0.23
$CCSCC + HO_2 \leftrightarrow CC^{\bullet}SCC + H_2O_2$	8.80E + 13	0.0	11120.0		0.27	0.44	0.48	
$CCSCC + OH \leftrightarrow C^{\bullet}CSCC + H_2O$	7.20E + 06	2.0	620.0	−2.0	−0.15	−0.54	−0.44	
$CCSCC + OH \leftrightarrow CC^{\bullet}SCC + H_2O$	3.80E + 06	2.0	300.0		0.19			
$CCSCC + O \leftrightarrow CC^{\bullet}SCC + OH$	6.80E + 09	1.5	4000.0	−2.0				
$CCS^{\bullet} \leftrightarrow CH_3 + CH_2{*}S$	8.61E + 12	0.8	42000.0				−0.82	
$CCS^{\bullet} + O_2 \leftrightarrow C_2H_5 + SO_2$	3.00E + 12	0.1	10414.0				0.83	
$CC^{\bullet}SH \leftrightarrow C^{\bullet}CSH$	5.10E + 12	0.0	40000.0				0.34	
$CH_3CH{*}S + OH \leftrightarrow H_2C{*}CHS^{\bullet} + H_2O$	1.08E + 07	2.0	700.0			−0.36		
$H + O_2 + N_2 \leftrightarrow HO_2 + N_2$	2.60E + 19	−1.2	0.0	5.2	−0.47	−0.83	−0.80	0.40
$H + O_2 \leftrightarrow OH + H$	2.65E + 16	−0.7	17041.0	−6.4	−0.52	1.48	1.2	0.66
$OH + HO_2 \leftrightarrow O_2 + H_2O$	1.45E + 13	0.0	−500.0	2.9				0.44
$HO_2 + CH_3 \leftrightarrow OH + CH_3O$	1.20E + 13	0.0	0.0	−2.3	−0.18	0.52	0.36	0.86
$H + C_2H_4 \leftrightarrow C_2H_5$	5.41E + 35	−6.8	11700.0		0.34	0.52	0.48	0.23
$OH + CH_2{*}O \leftrightarrow HCO + H_2O$	3.43E + 09	1.2	−447.0					−0.93
$O + C_2H_4 \leftrightarrow H + H_2C^{\bullet}CHO$	6.70E + 06	1.8	220.0		−0.16			
$OH + CH_3 \leftrightarrow CH_2(S) + H_2O$	6.44E + 17	−1.3	1417.0			0.47		
$O + C_2H_4 \leftrightarrow CH_3 + HCO$	1.25E + 07	1.8	220.0	1.6				0.30
$2CH_3 + M \leftrightarrow C_2H_6 + M$	6.77E + 16	−1.2	654.0					−0.30
$HCO + M \leftrightarrow H + CO + M$	1.87E + 17	−1.0	17000.0	−1.8				

A blank cell in the section of sensitivity coefficient indicates that the reaction does not occur among the top five reactions with high sensitivity for the species. Kinetic parameters are in modified Arrhenius format, $k = AT^n\exp(-E_a/RT)$, where A(mol, cm, s), $T(K)$, E_a(cal/mol), $R = 1.9859$ cal/mol K, n is dimensionless.

pre-exponential factor was calculated from the reverse association reaction of the two radicals and thermodynamics, which in turn was estimated from our evaluation of the well studied generic reaction: association of methyl radicals, adjusted for steric effects and degeneracy. The accuracy of a similar approach has been shown to be 30–35% for a different chemical system [39].

It is interesting that H abstraction from different carbons of diethyl sulfide and by different radicals shows opposite effects on the formation of products. As shown, the abstraction from the carbon attached to sulfur by OH can promote the formation of C_2H_4 as this reaction generates $CH_3CH{*}S + C_2H_5$. In contrast, C_2H_4 formation is inhibited by the abstraction by OH on the terminal carbon, as $C^{\bullet}CSCC$ reacts to $C_2H_4 + CCS^{\bullet}$, and this ethylthio radical reacts with the oxygenated species or undergoes β-scission to $CH_3{*}S + CH_3$. This difference can be explained by their net effects on the radical pools as the abstraction on the carbon attached to sulfur initializes a branch sequence to form H, while the abstraction on the terminal carbon converts OH and forms a less reactive stable CH_3. For SO_2 formation, two competing reactions involving ethylthio $CCS^{\bullet}$ have high sensitivity. The reaction of ethylthio $CCS^{\bullet}$ and O_2 is favored to increase SO_2 level as it produces SO_2 directly as well as C_2H_5, the dissociation of which increases the reaction rates of the whole system by increasing the level of H. A large part of the reactions with high sensitivities do not involve sulfur compounds, and these reactions are common radical branching, propagation, and termination reactions for hydrocarbon combustion systems.

5. Summary and conclusions

The oxidation of diethyl sulfide has been studied in an atmospheric, turbulent flow reactor at four temperatures between 630 and 740 °C. The initial chemical loadings included near-stoichiometric composition and fuel-lean composition with an equivalence ratio near 0.1. Complementary development of a chemical kinetic mechanism extended the published pyrolysis mechanism [9] by updating existing reactions and adding oxidation related pathways. Evolution of diethyl sulfide and its derivatives are modeled by more than 1000 reactions among about 300 species.

Experimental measurements and mechanism predictions are reported. The mechanism predictions reproduce the experimental results for CCSCC and C_2H_4 under all the studied conditions. For SO_2, CO and C_2H_6, the predictions are accurate under the fuel-lean conditions where these species were detected at high levels. Mechanism predictions have discrepancies with experimental data on minor species detected at low levels (<10 ppm) but reproduce the correct trends. Mechanism analysis shows that oxidation of

CCSCC is initiated through unimolecular dissociation. Once the radical pool is well established, H abstraction from CCSCC becomes an important destruction route. The resulting radicals undergo β-scission and subsequent oxidation steps to form C_2H_4, CO and SO_2. The radical branching, propagation and termination reactions, involving H, O and OH, are the reactions to which species concentrations are most sensitive.

The study shows that the presence of O_2 accelerates the destruction of CCSCC, which is fully expected. Significant intermediate products remain at the conditions studied, even with large excess O_2. The kinetics of major reaction intermediates, such as $CH_2{*}S$ and $CH_3CH{*}S$, are determined to be important. Further investigations involving direct measurements of these species would be highly desirable to provide a data set for improving the mechanism.

Acknowledgments

The authors acknowledge the support of the U.S. Army Research Office under contract W911NF0410120 and through instrument Grant DURIP W911NF0610142.

Appendix A. Supplementary data

Supplementary data associated with this article can be found, in the online version, at doi:10.1016/j.proci.2010.05.064.

References

[1] S.A. Carnes, A.P. Watson, *J. Am. Med. Assoc.* 262 (5) (1989) 653–659.
[2] Text of Chemical Weapons Convention, http://www.opcw.org/chemical-weapons-convention/.
[3] M.R. Green, *Am. J. Public Health* 93 (8) (2003) 1222–1226.
[4] P.A. Glaude, C. Melius, W.J. Pitz, C.K. Westbrook, *Proc. Combust. Inst.* 29 (2002) 2469–2476.
[5] J.H. Werner, T.A. Cool, *Combust. Flame* 117 (1999) 78–98.
[6] P.H. Taylor, B. Dellinger, C.C. Lee, *Environ. Sci. Technol.* 24 (1990) 316–328.
[7] D.V. Kozlov, A.V. Vorontsov, P.G. Smirniotis, E.N. Savinov, *Appl. Catal., B: Environ.* 42 (1) (2003) 77–87.
[8] A.V. Vorontsov, C. Lion, E.N. Savinov, P.G. Smirniotis, *J. Catal.* 220 (2) (2003) 414–423.
[9] X. Zheng, E.M. Fisher, F.C. Gouldin, L. Zhu, J.W. Bozzelli, *Proc. Combust. Inst.* 32 (2009) 469–476.
[10] X. Zheng, *Pyrolysis and Oxidation of Sulfur Mustard Simulants*, Ph.D. thesis, Cornell University, Ithaca, NY, USA, 2009.
[11] A.Y. Chang, J.W. Bozzelli, A.M. Dean, *Z. Phys. Chem.* 214 (2000) 1533–1568.
[12] L. Zhu, J.W. Bozzelli, *J. Phys. Chem. A* 110 (21) (2006) 6923–6937.
[13] L. Zhu, J.W. Bozzelli, in: *The 5th U.S. National Combustion Meeting*. Combustion Institute, San Diego, CA, 2007.
[14] L. Zhu, J.W. Bozzelli, *J. Mol. Struct.– THEOCHEM* 728 (2005) 147–157.
[15] R. Asatryan, J.W. Bozzelli, *Phys. Chem. Chem. Phys.* 10 (2008) 1769–1780.
[16] Sulfur mechanism, v5, 2002, available at http://www.chem.leeds.ac.uk/Combustion/sox.html.
[17] A.M. Dean, J.W. Bozzelli, *Gas Phase Combustion Chemistry*, Springer, New York, 1992, p. 138.
[18] C.Y. Sheng, J.W. Bozzelli, A.M. Dean, A.Y. Chang, *J. Phys. Chem. A* 106 (32) (2002) 7276–7293.
[19] C.J. Chen, J.W. Bozzelli, *J. Phys. Chem. A* 104 (21) (2000) 4997–5012.
[20] J. Lee, J.W. Bozzelli, *J. Phys. Chem. A* 107 (19) (2003) 3778–3791.
[21] C. Sheng, *Elementary, Pressure Dependence Model for Combustion of C1, C2 and Nitrogen Containing hydrocarbons: Operation of A Pilot Scale Incinerator and Model Comparison*, Ph.D. thesis, New Jersey Institute of Technology, Newark, NJ, USA, 2001.
[22] X. Zhong, J.W. Bozzelli, *J. Phys. Chem. A* 102 (20) (1998) 3537–3555.
[23] C.J. Chen, J.W. Bozzelli, *J. Phys. Chem. A* 103 (48) (1999) 9731–9769.
[24] W.C. Ing, *Reaction Kinetics on Methanol and MTBE Oxidation and Pyrolysis*, Ph.D. thesis, New Jersey Institute of Technology, Newark, NJ, USA, 1996.
[25] N. Sebbar, H. Bockhorn, J.W. Bozzelli, *Phys. Chem. Chem. Phys.* 4 (2002) 3691–3703.
[26] J.W. Bozzelli, C.Y. Sheng, *J. Phys. Chem. A* 106 (7) (2002) 1113–1121.
[27] T. Yamada, *The Oxidation of Dimethyl-Ether and ethylene in the atmosphere and Combustion Environment and Thermodynamic Studies on Hydrofluorocarbons Using Ab Initio Calculation Methods*, Ph.D. thesis, New Jersey Institute of Technology, Newark, NJ, USA, 1999.
[28] T. Yamada, J.W. Bozzelli, T.H. Lay, *Int. J. Chem. Kinet.* 32-7 (2000) 435–452.
[29] C.J. Montgomery, Q. Tang, A.F. Sarofim, M.J. Bockelie, J.K. Gritton, J.W. Bozzelli, F.C. Gouldin, E.M. Fisher, S. Chakravarthy, *Improved Kinetic Models for High-Speed Combustion Simulation*, Report No. AFRL-RZ-WP-TR-2008-2197, Air Force Research Laboratory, 2008.
[30] W.C. Ing, C.Y. Sheng, J.W. Bozzelli, *Fuel Process. Technol.* 83-1-3 (2003) 111–145.
[31] G.D. Silva, M.R. Hamdan, J.W. Bozzelli, *J. Chem. Theory Comput.* 5 (12) (2009) 3185–3194.
[32] J.W. Bozzelli, R. Asatryan, C.J. Montogomery, in: *The 5th U.S. National Combustion Meeting, Combustion Institute*, San Diego, CA, 2007
[33] M.U. Alzueta, R. Bilbao, P. Glarborg, *Combust. Flame* 127 (4) (2001) 2234–2251.
[34] W.J. Hehre, R. Ditchfield, L. Radom, J.A. Pople, *J. Am. Chem. Soc.* 92 (16) (1970) 4796–4870.
[35] T.H. Lay, J.W. Bozzelli, A.M. Dean, E.R. Ritter, *J. Phys. Chem.* 99 (1995) 14514–14527.
[36] Reaction Design, 2004, Chemkin User Interface 4.0, available at http://www.reactiondesign.com.

[37] W.S. Chin, B.W. Ek, C.Y. Mok, H.H. Huang, *J. Chem. Soc., Perkin Trans.* 2 (1994) 883–889.
[38] M.J. Pilling, S.H. Robertson, *Annu. Rev. Phys. Chem.* 54 (2003) 245–2275.
[39] I.A. Awan, D.R. Burgess, W. Tsang, J.A. Manion, Int. *J. Chem. Kinet.*, in press.